



HAL
open science

Raman scattering study of alpha-quartz and $\text{Si}(1-x)\text{Ge}_x\text{O}_2$ solid solutions

Vincent Ranieri, David Bourgogne, Stéphane Darracq, Martine Cambon,
Julien Haines, Olivier Cambon, Rozenn Le Parc, Claire Levelut, Alain
Largeteau, Gérard Demazeau

► **To cite this version:**

Vincent Ranieri, David Bourgogne, Stéphane Darracq, Martine Cambon, Julien Haines, et al.. Raman scattering study of alpha-quartz and $\text{Si}(1-x)\text{Ge}_x\text{O}_2$ solid solutions. *Physical Review B: Condensed Matter and Materials Physics (1998-2015)*, 2009, 79 (22), pp.224304. 10.1103/PhysRevB.79.224304 . hal-00434422

HAL Id: hal-00434422

<https://hal.science/hal-00434422>

Submitted on 14 Jun 2022

HAL is a multi-disciplinary open access archive for the deposit and dissemination of scientific research documents, whether they are published or not. The documents may come from teaching and research institutions in France or abroad, or from public or private research centers.

L'archive ouverte pluridisciplinaire **HAL**, est destinée au dépôt et à la diffusion de documents scientifiques de niveau recherche, publiés ou non, émanant des établissements d'enseignement et de recherche français ou étrangers, des laboratoires publics ou privés.

Raman scattering study of α -quartz and $\text{Si}_{1-x}\text{Ge}_x\text{O}_2$ solid solutionsV. Ranieri,^{1,*} D. Bourgoigne,² S. Darracq,³ M. Cambon,¹ J. Haines,¹ O. Cambon,^{1,†} R. Leparç,⁴ C. Levelut,⁴ A. Largeteau,³ and G. Demazeau³¹*Institut Charles Gerhardt de Montpellier, UMR 5253, CNRS-UM2-ENSCM-UM1, Université Montpellier 2, Equipe PMOF, cc1504, Place E. Bataillon, F-34095 Montpellier Cedex 5, France*²*Institut Charles Gerhardt de Montpellier, UMR 5253, CNRS-UM2-ENSCM-UM1, Université Montpellier 2, Equipe AIME, cc015, Place E. Bataillon, F-34095 Montpellier Cedex 5, France*³*Institut de Chimie de la Matière Condensée de Bordeaux, UPR 9048 CNRS, Université Bordeaux 1, Site de l'ENSCP, 87 Avenue du Dr. A. Schweitzer, 33608 Pessac Cedex, France*⁴*Laboratoire des Colloïdes, Verres et Nanomatériaux, UMR 5587, Université Montpellier 2, cc026, Place E. Bataillon, F-34095 Montpellier Cedex 5, France*

(Received 27 March 2009; revised manuscript received 2 June 2009; published 22 June 2009)

α -quartz-type $\text{Si}_{1-x}\text{Ge}_x\text{O}_2$ solid solutions ($x=0.06, 0.11,$ and 0.24) and pure SiO_2 were investigated by Raman spectroscopy. Coupled and decoupled vibrational modes were identified at room temperature as a function of composition. Tetrahedral tilting librational modes involved in the displacive $\alpha \leftrightarrow \beta$ -quartz phase transition are decoupled. The wave number of the coupled A_1 mode located at 464 cm^{-1} for pure α -quartz was found to vary quite linearly with germanium content. Raman spectra were recorded up to 1473 K. Substitution of germanium in the quartz lattice clearly improves the thermal stability of the α phase. The $\alpha \leftrightarrow \beta$ -quartz phase transition temperature increases from $846 \pm 1 \text{ K}$ for $x=0$ to about $1300 \pm 50 \text{ K}$ for $x=0.24$. At the same time, the dynamic disorder observed in quartz well below the transition is reduced in the solid solutions.

DOI: [10.1103/PhysRevB.79.224304](https://doi.org/10.1103/PhysRevB.79.224304)

PACS number(s): 63.20.-e, 65.40.-b, 61.66.Fn, 61.50.-f

I. INTRODUCTION

Silicon dioxide is of great importance for earth and materials science, crystal chemistry, and solid-state physics. The study of analog materials and solid solutions between them (GeO_2 , BeF_2 , PON, and ABO_4 , where $A=B, \text{Al, Ga, Fe; } B=\text{P, As}$) provides models for SiO_2 and materials with potentially improved properties for various applications. The stable form of silicon dioxide under ambient conditions is trigonal α -quartz. At high-temperature α -quartz transforms successively to β -quartz, HP-tridymite, β -cristobalite and finally melts to form liquid silica at 2000 K.¹ The nature of the displacive $\alpha \leftrightarrow \beta$ transition in quartz has been the subject of numerous studies.¹⁻⁷ “Soft mode behavior”⁸⁻¹³ has also been related to tetrahedral tilting in these materials, but recent work indicates that the transition mechanism is more complex involving dynamic disorder.^{14,15} The high-temperature β -phases of silicon dioxide polymorphs are characterized by a significant degree of dynamic disorder linked to excited rigid-unit modes (RUMs).^{7,14,16-18} This disorder appears well below the $\alpha \leftrightarrow \beta$ transition temperature^{14,19} and has an important impact on materials properties such as piezoelectricity.^{19,20}

Silicon dioxide is one of the most extensively studied solid materials by vibrational spectroscopy. The first experiments on the α -quartz phase were reported in 1940 by Raman and Nedungadi.⁸ The complete assignment of the A_1 and E optical modes were made by polarized-Raman experiments.¹⁰ The temperature dependence of the α -quartz Raman spectrum has been the subject of numerous studies.^{8,9,21-26} The displacive $\alpha \leftrightarrow \beta$ phase transition can be recognized based on the wave-number shifts and the changes in the full width at half maximum (FWHM) of the A_1 mode located at 464 cm^{-1} corresponding to the bending vibrations

of the intratetrahedral O-Si-O angles^{26,27} and also by the disappearance of the 355 cm^{-1} A_1 mode. Less work has been performed on GeO_2 .^{11,24,28-30} Raman spectra of the trigonal form analogous to α -quartz were first reported by Scott¹¹ with the assignment of all bands. This assignment was subsequently revised by Dultz *et al.*³¹ and some A and E mode assignments at low wave number were modified. Compared to the spectra of α -quartz, most of the bands are shifted to lower wave number due to the difference in mass between Si and Ge atoms. The thermal stability was investigated by several experiments,^{23,29,30} no $\alpha \leftrightarrow \beta$ phase transition was observed for this material. GeO_2 is stable at higher temperature than any other α -quartz homeotype and is one of the most distorted materials with respect to the β -quartz-type structure.^{32,33} Correlation between the structural distortion, thermal stability, and some physical, dielectric, and piezoelectric properties with respect to the β -quartz structure type have been established for α -quartz homeotypes.³²⁻⁴² In this family of materials, distortion can be described by the inter-tetrahedral bridging angle θ and the tetrahedral tilt angle δ , which is the order parameter for the $\alpha \leftrightarrow \beta$ phase transition.⁴³ Thus, substituting a larger cation in the α -quartz piezoelectric phase could be a promising way to improve the physical properties.

Few studies on the crystalline SiO_2 - GeO_2 system have been reported in the literature. The maximum miscibility observed by Miller *et al.*⁴⁴ for germanium in the SiO_2 α -quartz lattice is about 31 at. % beyond which an additional GeO_2 rutile-type phase appears. In addition to the establishment of structure-property relationships cited above interest was focused on hydrothermal growth of single crystals⁴⁵ in order to obtain higher performance α -quartz homeotype piezoelectric materials. Due to the difference of solubility between SiO_2 and GeO_2 , growth of homogeneous single crystals is complex and the study of polycrystalline materials^{44,46,47} may

improve our knowledge of the physical properties of this system. Raman spectroscopy is a powerful technique to study the disorder and thermal stability of solid solutions. Recent work on α -quartz-type $\text{Al}_{1-x}\text{Ga}_x\text{PO}_4$ solid solutions indicates that Raman spectra are modified by Ga-Al substitution.⁴⁸ Two types of modes were identified: coupled modes that vary continuously in wave number with x and decoupled modes that are inherent either to AlO_4 or GaO_4 tetrahedra and do not appear in the spectrum of the opposite end member. The broadening at high temperature of the decoupled mode linked to tetrahedral librations increases more rapidly in the Al-rich compounds, indicating that dynamic disorder appears at lower temperature for these compositions. The present study was undertaken to investigate the influence of germanium substitution on the Raman spectra and on the $\alpha \leftrightarrow \beta$ phase transition of quartz.

II. EXPERIMENTAL

A. Samples preparation

$\text{Si}_{1-x}\text{Ge}_x\text{O}_2$ powders with the α -quartz-type structure were synthesized in two steps: (i) synthesis of a gel from a mixture of alkoxides and (ii) crystallization via a solvothermal treatment.⁴⁷ The structure of the synthesized powder samples was determined by x-ray powder diffraction measurements performed on a PANalytical X'Pert diffractometer equipped with an X'celerator detector using a Ni-filtered $\text{Cu } K\alpha$ radiation.

Mixed single crystals ($x < 0.20$) were grown by the hydrothermal method. These crystals were used to determine the correlation between the Ge content measured by electron probe microanalysis instrument (EPMA) and the wave-number shift observed in Raman spectra.

The composition was measured using a CAMECA SX100 EPMA and Raman spectroscopy. It will be shown that for a solid solution such as $\text{Si}_{1-x}\text{Ge}_x\text{O}_2$ Raman spectroscopy is a convenient alternative to EPMA avoiding tedious sample preparation (see Sec. III A).

B. Measurements

Raman spectra were obtained using a Horiba Jobin-Yvon LabRam Aramis Raman spectrometer equipped with a blue diode laser ($\lambda = 473$ nm), an Olympus microscope, and a charge coupled device camera cooled by a thermoelectric Peltier device. The laser power was about 20 mW on the sample. A ground pure SiO_2 α -quartz single crystal and the $\text{Si}_{1-x}\text{Ge}_x\text{O}_2$ solid solution were placed on a thin platinum block in the oven of a Linkam TS1500 heating stage under the objective (X50) of the microscope. The temperature was measured by a thermocouple at the bottom of the oven and checked during the experiment using the ground synthetic α -quartz sample for which $\alpha \leftrightarrow \beta$ transition temperature is well known (846 K) as a reference. The spectrometer was calibrated using a Si sample.

High-temperature x-ray powder diffraction measurements were performed on a PanAnalytical X'Pert diffractometer equipped with an X'celerator detector using Ni-filtered, $\text{Cu } K\alpha$ radiation. The powder samples were placed in the

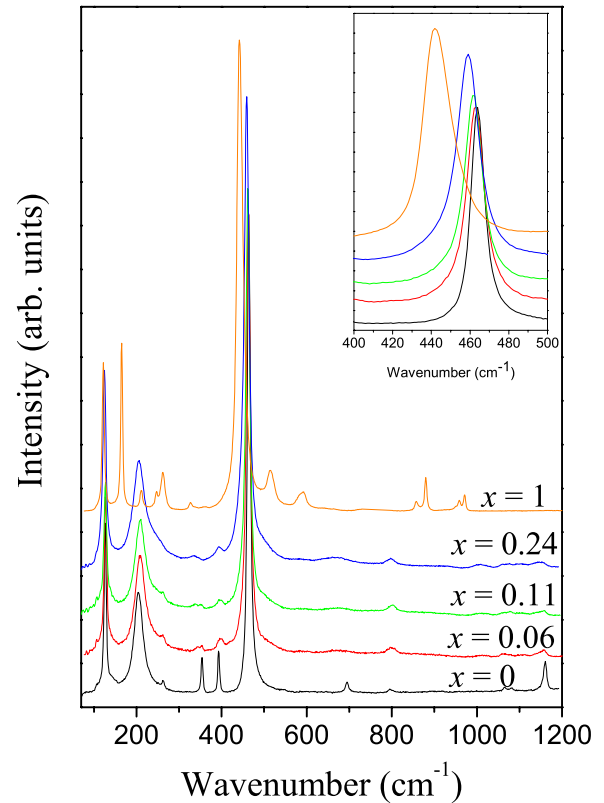


FIG. 1. (Color online) Raman spectra of α -quartz-type $\text{Si}_{1-x}\text{Ge}_x\text{O}_2$ as a function of composition

ceramic spinning sample holder of an Anton Paar HTK 1200 high-temperature oven chamber. X-ray diffraction data were obtained from 19° to 124° in 2θ with 0.008° step size over the temperature range up to 1073 K.

III. RESULTS AND DISCUSSION

A. Room-temperature spectra of $\text{Si}_{1-x}\text{Ge}_x\text{O}_2$

The two end members α -quartz SiO_2 and α -quartz-type GeO_2 are trigonal $P3_121$ (symmetry D_3) with Si/Ge atoms located in the center of corner-shared (Si/Ge) O_4 tetrahedra. Group theory predicts the following representation of the optical vibrations:

$$\Gamma_{\text{op}} = 4A_1 + 4A_2 + 8E$$

There are 12 modes predicted to be Raman active, four non-degenerate A_1 , and eight doubly-degenerate E . The degenerate E modes can be split into transverse optical (TO) and longitudinal optical (LO) components by the interaction of long-range forces within the crystal.

For a solid solution such as $\text{Si}_{1-x}\text{Ge}_x\text{O}_2$, the observed modes involving Si/Ge atoms may be coupled leading to one mode varying in wave number as a function of composition between the two end members or decoupled leading to localized modes arising from vibrations of the SiO_4 or GeO_4 tetrahedra not present in the opposite end members.⁴⁸

Raman spectra of several compositions from $x=0$ to $x=1$ were obtained (Fig. 1). All bands were fitted using a

TABLE I. Raman modes (cm^{-1}) of α -quartz-type $\text{Si}_{1-x}\text{Ge}_x\text{O}_2$ as a function of composition (note that coupled modes are in *italics*; vw=very weak; and sh=shoulder).

Modes	$x=0$	$x=0.06$	$x=0.11$	$x=0.14$	$x=0.24$	$x=1$
<i>E(TO+LO)</i>	126	127	127	125	124	123
<i>E(TO+LO)</i>						166
A_1	204	209	209	207	206	
<i>E(TO+LO)</i>						212
<i>E(TO+LO)</i>	263	256	262	258	sh	
<i>E(TO+LO)</i>						247
A_1						263
A_1					331	328
A_1	354	353	351	352		
E (TO)	392	398	396	392	407	
E (TO)	449					
A_1	464	462.7	461.6	461	458.9	443
E (LO)						516
E (TO)						585
E (LO)						595
<i>E(TO+LO)</i>	695	vw	vw	vw	vw	
E (TO)	795	799	801	800	797	
E (TO)						858
A_1						880
E (LO)						950
E (TO)						959
E (LO)						971
E (TO)	1065					
A_1	1081	vw	vw	vw	vw	
<i>E(TO+LO)</i>	1158	1155	1157	1157	vw	

pseudo-Voigt function. Spectra of $\text{Si}_{1-x}\text{Ge}_x\text{O}_2$ powders ($x_{\text{max}}=0.24$) are similar to the spectrum of the ground α -quartz single crystal. The substitution of Si atoms by heavier Ge atoms alters the wave number of vibrations in which these atoms take part (Table I). As expected, coupled modes shift to lower wave number with the substitution. These modes are located in the low wave-number region (close to 126 cm^{-1}), corresponding to complex bending and twisting of $(\text{Si}/\text{Ge})\text{O}_4$ tetrahedra and midwave-number region (between 440 and 465 cm^{-1}) corresponding to O-(Si/Ge)-O bending vibrations.²⁷ Modes in the high wave-number region (above 700 cm^{-1}) are decoupled and correspond to Si-O and Ge-O internal stretching modes of the SiO_4 and the GeO_4 tetrahedra. In this region, a large decrease in amplitude is observed with Ge-Si substitution and it became difficult to assign some modes, especially for the compound with 24 at. % of germanium. The wave-number shift of the coupled modes is quite small with respect to the mass difference between Si and Ge atoms indicating that these vibrations are principally due to the motion of oxygen atoms. Another important decoupled mode is the tetrahedral librational mode at 206 cm^{-1} for $x=0$. A comparative study between EPMA and Raman scattering measurements on single crystals ($x < 0.20$) indicates that the shift of the intratetrahedral O-(Si/Ge)-O bending vibration can be used to determine

the Ge content. This mode located at 464 cm^{-1} for α -quartz ($x=0$) and 443 cm^{-1} for α -quartz-type GeO_2 shifts almost linearly [Fig. 2(a)] between the two end members and the composition can be estimated using the following expression:

$$\nu(\text{cm}^{-1}) = 464.064 - 0.21x_{\text{Ge}}$$

Moreover, a significant increase of the linewidth also appears [Fig. 2(b)] with substitution. The broadening can be linked to structural disorder due to the different environments around Si and Ge and the presence of Si-O-Si, Ge-O-Ge, and Si-O-Ge linkages.

B. High-temperature measurements

The decomposition of optical modes into irreducible representations of the β -quartz phase is described by:

$$\Gamma_{\text{op}} = A_1 + 3B_1 + 2A_2 + 2B_2 + 4E_1 + 4E_2$$

The B_1 , B_2 , and A_2 modes are Raman inactive, thus, only nine modes, one nondegenerate, and eight doubly degenerate are Raman active in the β phase.

Four different compositions from $x=0$ to $x=0.24$ of $\text{Si}_{1-x}\text{Ge}_x\text{O}_2$ were studied at high temperature up to 1373 K in order to determine the influence of Ge-Si substitution on the

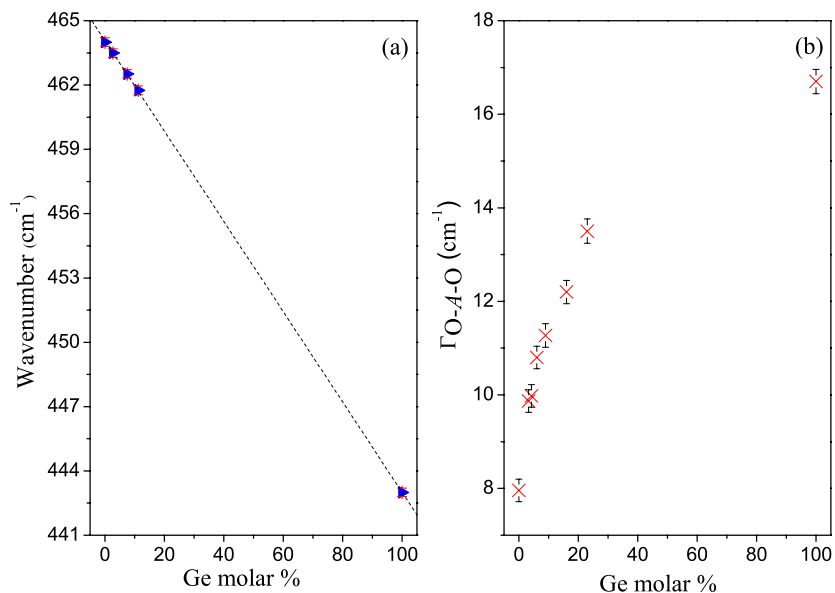


FIG. 2. (Color online) (a) Correlation between Raman shift of the O-A-O vibration and Ge molar fraction measured by EPMA on single crystal samples ($x < 0.20$); (b) Composition dependence of the full width at half maximum of the O-A-O vibration line

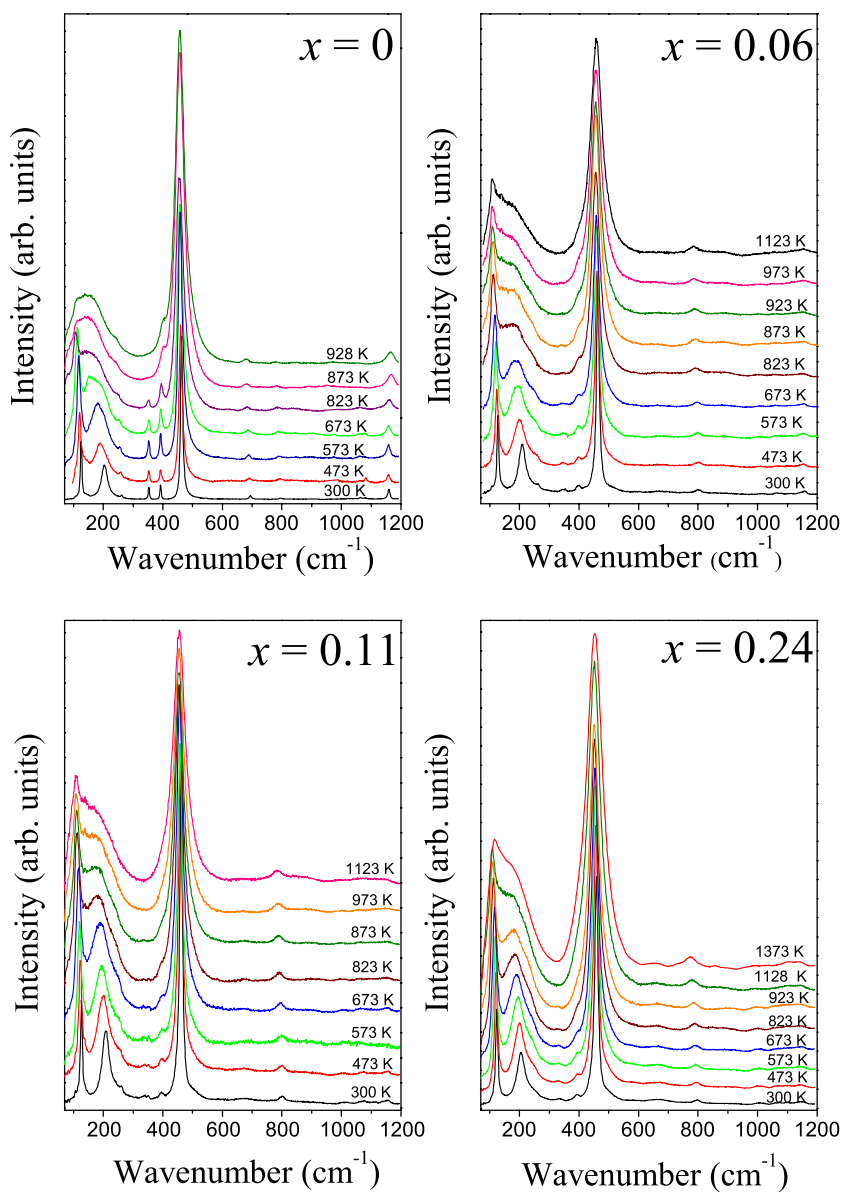


FIG. 3. (Color online) High-temperature Raman spectra of $\text{Si}_{1-x}\text{Ge}_x\text{O}_2$ ($x = 0; 0.06; 0.11; 0.24$)

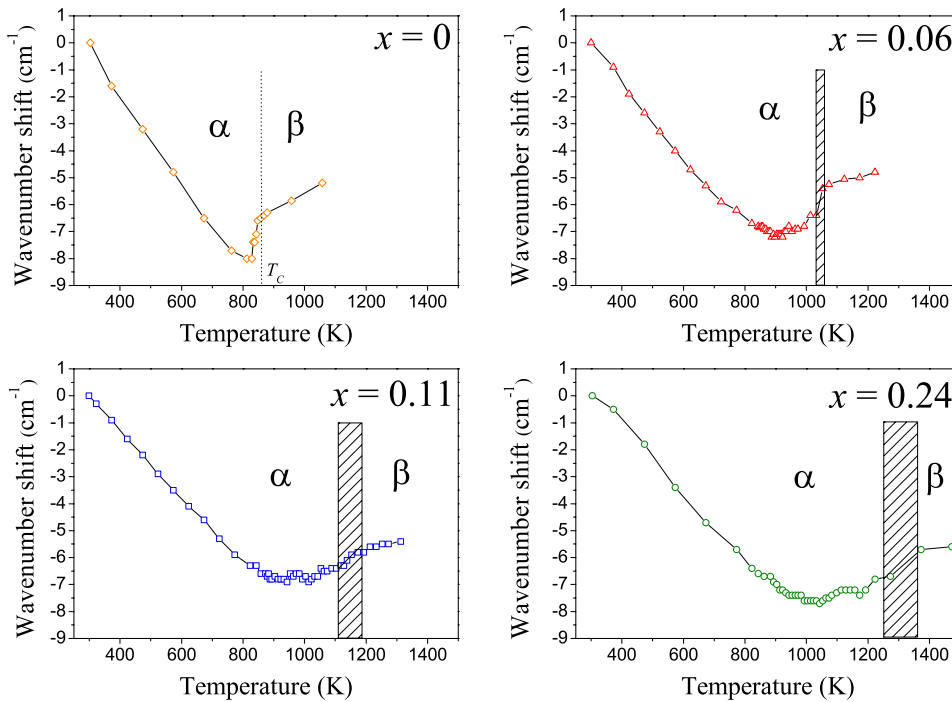


FIG. 4. (Color online) Wave-number shift with temperature of the O-A-O vibration band of $\text{Si}_{1-x}\text{Ge}_x\text{O}_2$ ($x=0, 0.06, 0.11,$ and 0.24). The transition temperature for $x=0$ (dotted line) and the solid solutions (shaded region) are indicated.

vibrational properties and the stability of the α -quartz-type phase in these materials.

1. Phase transition in α -quartz SiO_2

The evolution of the Raman spectra is presented in Fig. 3. A progressive change in wave number and linewidth of Raman modes is observed over the temperature range up to 1073 K (Figs. 4 and 5). The displacive $\alpha \leftrightarrow \beta$ phase transition occurs at $T_c=846$ K for α -quartz ($x=0$). This structural phase transition can be evidenced by the disappearance of

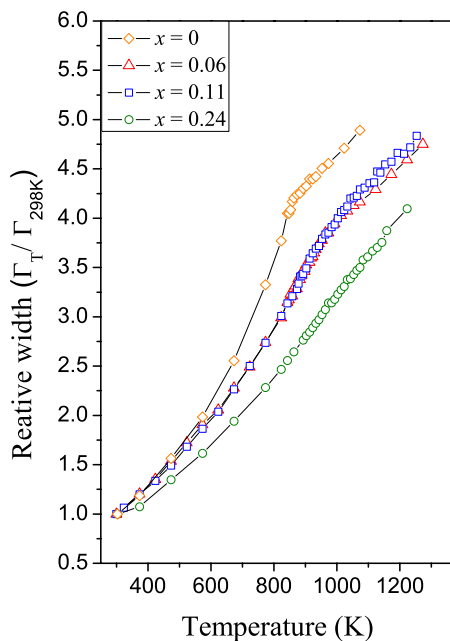


FIG. 5. (Color online) Temperature dependence of the relative peak width of the O-A-O bending vibration band

the $354 \text{ cm}^{-1} A_1$ mode and the change in both wave-number shift and linewidth of the slightly anharmonic 464 cm^{-1} O-Si-O intratetrahedra bending vibrational mode²²⁻²⁷ (Figs. 4 and 5). Three different trends can be noted in the wave-number shift of this line before the transformation to β -quartz: (i) an almost linear wave number decrease from room temperature to about 815 K, (ii) the wave number remains nearly constant until 830 K, and (iii) approaching the phase transition the wave number increases quickly (1.5 cm^{-1} over 20 K). A discontinuity occurs at the $\alpha \leftrightarrow \beta$ phase transition and the increase in wave number became linear in the β -quartz phase. The linewidth of the 464 cm^{-1} mode broadens from 8 cm^{-1} at room temperature to about 40 cm^{-1} at 1073 K. The broadening displays a discontinuity at the $\alpha \leftrightarrow \beta$ -quartz transition.

The lattice instability of quartz is expressed by the “soft modes” located at 128 and 206 cm^{-1} having strong temperature dependence. The behavior of the 206 cm^{-1} mode corresponding to SiO_4 tetrahedral librations is very interesting. This mode is strongly anharmonic,^{24,25} both its wave number and linewidth present a strong temperature dependence. The initial wave number shifts from 206 to 176 cm^{-1} over 500 K and its linewidth increases in a nonlinear way. The broadening increases above 570 K up to T_c . A total neutron scattering study shown that the degree of structural disorder increases well below the displacive $\alpha \leftrightarrow \beta$ phase transition.^{14,19} The distribution of O-O-O intertetrahedral angles is well defined at room temperature but broadens rapidly from 473 K and becomes very broad at 673 K indicating that SiO_4 tetrahedra are randomly oriented. The damping of the decoupled tetrahedral librations 206 cm^{-1} mode can be linked to this random orientation of SiO_4 tetrahedra.

2. Phase transition in α -quartz-type $\text{Si}_{1-x}\text{Ge}_x\text{O}_2$ solid solution

Raman spectra of three α -quartz-type $\text{Si}_{1-x}\text{Ge}_x\text{O}_2$ ($x=0.06, 0.11,$ and 0.24) samples as a function of temperature

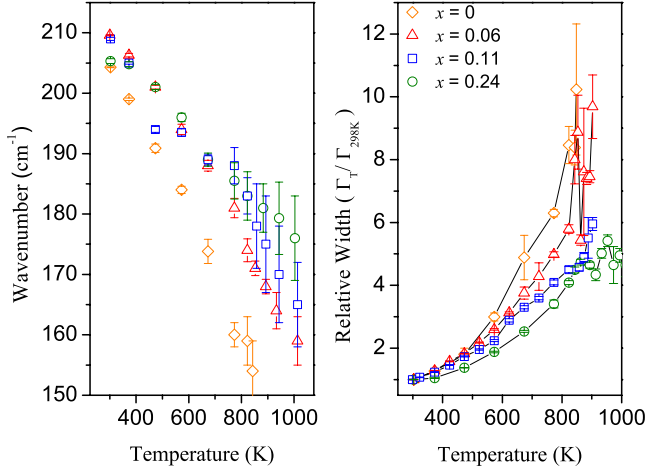


FIG. 6. (Color online) Temperature dependence of the wave number and the relative peak width of the “soft mode” located around 206 cm^{-1} .

are compared to α -quartz in Fig. 3. Globally, the high-temperature behavior of the solid solutions is similar to that of pure SiO_2 . Due to the high degree of damping, the disappearance of the 354 cm^{-1} A_1 mode became too difficult to detect, so the displacive $\alpha \leftrightarrow \beta$ phase transition can be identified only via the wave-number shift and the change in the full width at half maximum of the O-A-O ($\Gamma_{\text{O-A-O}}$) bending vibration (Figs. 4 and 5). The three trends reported for α -quartz are also observed, but following the linear decrease, the wave number remains almost constant over a wide range of temperature for the solid solutions. In fact, there is no evidence for (Si/Ge) ordering in the structure. The trigonal structure contains three (Si/Ge) atoms per unit cell; the reported composition is an average value over several unit cells. Therefore, the observed phase transition corresponds to a series of transitions occurring for different compositions at slightly different temperatures and the low-temperature α phase and the high-temperature β phase coexist over a large range of temperature. The wide temperature range over which the phase transition occurs can also be clearly seen from the evolution of the $\Gamma_{\text{O-A-O}}$ (Fig. 5). The clear discontinuity occurring at the transition in α -quartz SiO_2 disappears in the solid solution. It is still possible to observe a slight change in curvature for $x=0.06$ and $x=0.11$, but this change occurs over a large range of temperature in good agreement with the behavior of the shift in wave number of the O-A-O mode described above. The soft mode (206 cm^{-1}) involved in the displacive $\alpha \leftrightarrow \beta$ phase transition is strongly affected by the Ge content. The temperature dependence of this mode decreases with the amount of germanium (Fig. 6). A 44 cm^{-1} wave-number shift is observed for $x=0$ over a 470 K range whereas this shift decreases to 20 cm^{-1} for $x=0.24$. At the same time, the phonon lifetime decreases less rapidly with temperature in the solid solution and the line broadening is limited.

The total transformation to the β -quartz-type phase occurs at about $1045 \pm 15 \text{ K}$ for $x=0.06$, $1150 \pm 30 \text{ K}$ for $x=0.11$ and $1300 \pm 50 \text{ K}$ for $x=0.24$ with respect to the $846 \pm 1 \text{ K}$ for $x=0$.

TABLE II. Temperature shifts of the two “soft mode” (126 and 206 cm^{-1}), the strongest A_1 mode and the isobaric mode Grüneisen parameters as a function of x

Composition	$\tilde{\nu}_i$ (cm^{-1})	$\delta\tilde{\nu}_i/\delta T$ (cm^{-1}/K)	$\delta\tilde{\nu}_i/\delta T^a$ (cm^{-1}/K)	γ_i
$x=0$	126	-0.036	-0.036	4.2
	206	-0.086	-0.065	7
	464	-0.015	-0.014	0.6
$x=0.06$	127.5	-0.030		
	209.5	-0.068		
	462.7	-0.013		
$x=0.11$	126.5	-0.028		
	209	-0.050		
	461.6	-0.012		
$x=0.24$	123.5	-0.022		3.9
	205	-0.042		4.4
	458	-0.012		0.49

^aData from Gillet *et al.* (Ref. 24).

3. Thermal stability and disorder

In order to understand the improvement of the thermal stability of the material, it is important to extract the anharmonic contribution to the temperature dependence of the phonon wave number. The temperature dependence of the phonon wave number corresponds to the sum of an explicit and an implicit contribution, which are respectively a pure temperature contribution (self-anharmonic) and a pure volume contribution (thermal expansion).

$$\left(\frac{d\tilde{\nu}_i}{dT}\right)_P = \left(\frac{d\tilde{\nu}_i}{dT}\right)_{\text{explicit}} + \left(\frac{\partial\tilde{\nu}_i}{\partial V}\right)_T \left(\frac{dV}{dT}\right)_P \quad (1)$$

The phonon wave-number shift due to the implicit contribution of a given mode can be expressed as a function of the unit-cell volume introducing the quasiharmonic mode Grüneisen parameter (i.e., $\gamma_i = \gamma_{iP} = \gamma_{iT}$) as follows:⁴⁹

$$\gamma_i = -\frac{d \ln \tilde{\nu}_i}{d \ln V} = -\frac{V d\tilde{\nu}_i}{\tilde{\nu}_i dV} \quad (2)$$

The implicit part of the wave-number shift is given by the expression

$$\tilde{\nu}_i(T)_{\text{implicit}} = \tilde{\nu}_i(T=0) \left[\frac{V(T=0)}{V(T)} \right]^{\gamma_i} \quad (3)$$

For SiO_2 α -quartz, thermal expansion of the lattice is well known,³ the unit-cell volume and the wave number of the i th mode at 0 K are determined by extrapolation. Thermal expansion of the solid solution ($x=0.24$) was determined by high-temperature x-ray powder diffraction from room temperature up to 1073 K . The temperature dependence and the mode Grüneisen parameters of the soft modes and the strongest A_1 mode of Raman spectra are listed in Table II. Our data for α -quartz are in good agreement with the literature, the difference found for the temperature dependence of the 206 cm^{-1} soft mode can be attributed to the difficulty of

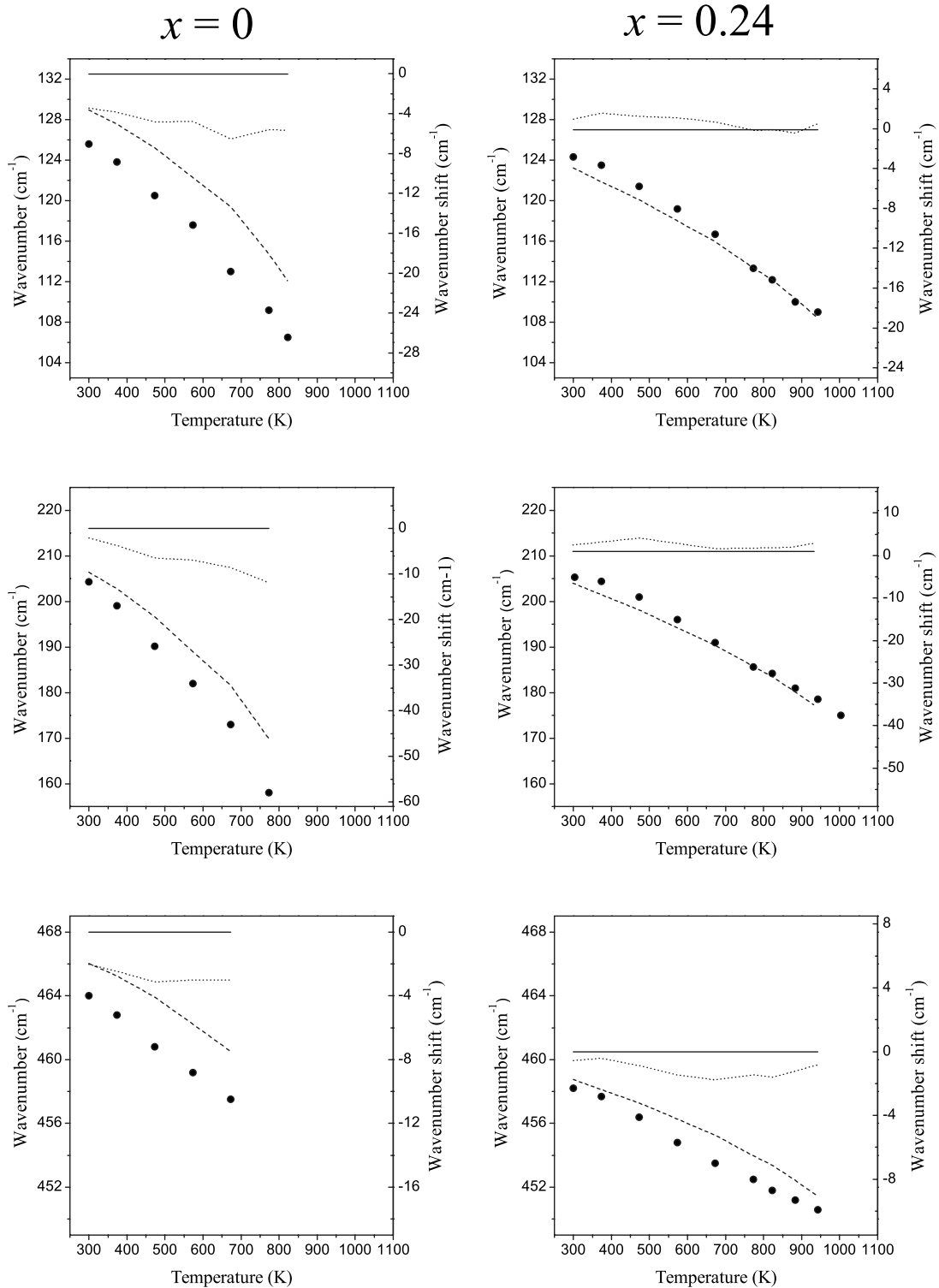


FIG. 7. Implicit and explicit contributions to the temperature dependence of the E and A_1 soft modes (top) and the strongest Raman A_1 line (bottom) of $\text{Si}_{1-x}\text{Ge}_x\text{O}_2$ ($x=0$ and 0.24). Black circles are experimental data points; dashed line the implicit contribution; dotted line the explicit contribution to the wave-number shift and black line wave number at $T=0$ K.

fitting this mode above 473 K because of significant broadening. The mode Grüneisen parameters are calculated from our isobaric data for $x=0$ and $x=0.24$ using the Eq. (2) and our volume data for $x=0.24$ and those from Carpenter *et al.*³ for $x=0$. In order to directly compare the two materials in a qualitative manner (quasiharmonic approximation), isobaric

data were used instead of isothermal data as no high-pressure data are available for $x=0.24$. The γ_i parameter is usually taken as being temperature independent, but due to the behavior of the modes approaching the $\alpha \leftrightarrow \beta$ phase transition, data obtained from 300 and 773 K for $x=0$ and from 300 and 1003 K for $x=0.24$ were used to calculate γ_i . Over these

temperature ranges, $(d \ln \tilde{\nu}_i / d \ln V)$ is linear. The temperature dependence and the γ_i of the three modes decrease with the Ge content from $x=0$ to $x=0.24$ (Table II), especially the tetrahedra librational A_1 soft mode.

The extraction of the thermal expansion contribution to the phonon wave-number shift enables us to clearly show the increase in stability of the materials containing germanium. The temperature dependence of three modes, for $x=0$ and $x=0.24$, with their implicit and explicit contribution is presented in Fig. 7. The self-anharmonic term plays an important role in the phonon wave-number shift of the α -quartz. The 206 cm^{-1} mode shift depends initially on thermal expansion, then from 420 K the slope of implicit contribution changes. The explicit contribution slightly increases up to 700 K and plays a more important role above 700 K. The solid solution exhibits a different behavior; the principal contribution to the phonon wave-number shift is due to thermal lattice expansion even at high temperature.

These results clearly show that the incorporation of germanium in the α -quartz structures results in a material which exhibits less dynamic disorder at high temperature. Additionally, the germanium substitution in the crystalline lattice should increase the structural distortion leading to an improvement in thermal stability that is clearly demonstrated in this paper and also to better piezoelectric properties in agreement with structure-properties relationships.³²⁻⁴²

IV. CONCLUSION

$\text{Si}_{1-x}\text{Ge}_x\text{O}_2$ solid solutions with the α -quartz-type structure were investigated by Raman scattering in order to understand the influence of Ge-Si substitution. At room temperature, change in wave number of the coupled A_1 Raman mode at 464 cm^{-1} for $x=0$ has been correlated with the Ge content. The wave-number shift and peak width were also determined from room temperature up to 1473 K. This investigation provides important information on the structural stability of the α -quartz-type form. The $\alpha \leftrightarrow \beta$ transition temperature increases with the germanium content x and occurs at about $1045 \pm 15 \text{ K}$ and up to $1300 \pm 50 \text{ K}$ for $x=0.06$ and $x=0.24$ respectively. All Raman bands broaden considerably with temperature especially the tetrahedral libration mode, which is linked to high degree of dynamic disorder. The explicit contribution to the wave-number shift is found to strongly decrease with germanium content. The thermal stability of the solid solutions is greatly improved and the dynamic disorder is reduced with respect to α -quartz.

ACKNOWLEDGMENT

The authors thank the French Ministry of Defense for financial support (Contract No. 05 34 051).

*vranieri@lpmc.univ-montp2.fr

†Corresponding author; ocambon@lpmc.univ-montp2.fr.

¹P. J. Heaney, *Rev. Mineral.* **29**, 1 (1994).

²G. Dolino, *Phase Transitions* **21**, 59 (1990).

³M. A. Carpenter, E. K. H. Salje, A. Graeme-Barber, B. Wruck, M. T. Dove, and K. S. Knight, *Am. Mineral.* **83**, 2 (1998).

⁴T. Demuth, Y. Jeanvoine, J. Hafner, and J. G. Ángyán, *J. Phys.: Condens. Matter* **11**, 3833 (1999).

⁵M. H. Müser, *J. Chem. Phys.* **114**, 6364 (2001).

⁶M. T. Dove, M. Gambhir, and V. Heine, *Phys. Chem. Miner.* **26**, 344 (1999).

⁷D. A. Keen and M. T. Dove, *J. Phys.: Condens. Matter* **11**, 9263 (1999).

⁸C. V. Raman and T. M. Nedungadi, *Nature (London)* **145**, 147 (1940).

⁹S. M. Shapiro, D. C. O'Shea, and H. Z. Cummins, *Phys. Rev. Lett.* **19**, 361 (1967).

¹⁰J. F. Scott, *Phys. Rev. Lett.* **21**, 907 (1968).

¹¹J. F. Scott, *Phys. Rev. B* **1**, 3488 (1970).

¹²J. F. Scott, *Rev. Mod. Phys.* **46**, 83 (1974).

¹³T. Shigenari, Y. Imura, and Y. Takagi, *J. Phys. Soc. Jpn.* **49**, (Suppl. B), 29 (1980).

¹⁴M. G. Tucker, D. A. Keen, and M. T. Dove, *Mineral. Mag.* **65**, 489 (2001).

¹⁵I. Gregora, N. Magneron, P. Simon, Y. Luspin, N. Raimboux, and E. Philippot, *J. Phys.: Condens. Matter* **15**, 4487 (2003).

¹⁶M. T. Dove, V. Heine, and K. D. Hammonds, *Mineral. Mag.* **59**, 629 (1995).

¹⁷M. G. Tucker, M. T. Dove, and D. A. Keen, *J. Phys.: Condens.*

Matter **12**, L723 (2000).

¹⁸S. A. Wells, M. T. Dove, M. G. Tucker, and K. Trachenko, *J. Phys.: Condens. Matter* **14**, 4645 (2002).

¹⁹J. Haines, O. Cambon, D. A. Keen, M. G. Tucker, and M. T. Dove, *Appl. Phys. Lett.* **81**, 2968 (2002).

²⁰J. Haines, O. Cambon, N. Prud'homme, G. Frayssé, D. A. Keen, L. C. Chapon, and M. G. Tucker, *Phys. Rev. B* **73**, 014103 (2006).

²¹J. B. Bates and A. S. Quist, *J. Chem. Phys.* **56**, 1528 (1972).

²²K. J. Dean, W. F. Sherman, and G. R. Wilkinson, *Spectrochim. Acta, Part A* **38**, 1105 (1982).

²³S. K. Sharma, *Vib. Spectra Struct.* **17B**, 513 (1989).

²⁴Ph. Gillet, A. Le Cléach, and M. Madon, *J. Geophys. Res.* **95**, 21635 (1990).

²⁵J. Castex and M. Madon, *Phys. Chem. Miner.* **22**, 1 (1995).

²⁶C. Schmidt and M. A. Ziemann, *Am. Mineral.* **85**, 1725 (2000).

²⁷J. Etchepare, M. Merian, and L. Smetankine, *J. Chem. Phys.* **60**, 1873 (1974).

²⁸L. P. Avakyants, D. F. Kiselev, I. B. Makhina, and M. M. Firsova, *Opt. Spectrosc.* **66**, 541 (1989).

²⁹M. Madon, Ph. Gillet, Ch. Julien, and G. D. Price, *Phys. Chem. Miner.* **18**, 7 (1991).

³⁰T. P. Mernagh and L-g. Liu, *Phys. Chem. Miner.* **24**, 7 (1997).

³¹W. Dultz, M. Quilichini, J. F. Scott, and G. Lehman, *Phys. Rev. B* **11**, 1648 (1975).

³²E. Philippot, A. Goiffon, A. Ibanez, and M. Pintard, *J. Solid State Chem.* **110**, 356 (1994).

³³J. Haines, O. Cambon, E. Philippot, L. Chapon, and S. Hull, *J. Solid State Chem.* **166**, 434 (2002).

- ³⁴O. Cambon, P. Yot, S. Ruhl, J. Haines, and E. Philippot, *Solid State Sci.* **5**, 469 (2003).
- ³⁵J. Haines, O. Cambon, and S. Hull, *Z. Kristallogr.* **218**, 193 (2003).
- ³⁶J. Haines, C. Chateau, J. M. Léger, and R. Marchand, *Ann. Chim. Sci. Mat.* **26**, 209 (2001).
- ³⁷E. Philippot, D. Palmier, M. Pintard, and A. Goiffon, *J. Solid State Chem.* **123**, 1 (1996).
- ³⁸E. Philippot, P. Armand, P. Yot, O. Cambon, A. Goiffon, G. J. McIntyre, and P. Bordet, *J. Solid State Chem.* **146**, 114 (1999).
- ³⁹O. Cambon and J. Haines, *Proceedings of 2003 IEEE International Frequency Control Symposium in the 17th European Frequency Time Forum* (IEEE, Piscataway, NJ, 2003), p. 650.
- ⁴⁰J. Haines, O. Cambon, R. Astier, P. Fertey, and C. Chateau, *Z. Kristallogr.* **219**, 32 (2004).
- ⁴¹J. Haines and O. Cambon, *Z. Kristallogr.* **219**, 314 (2004).
- ⁴²O. Cambon, J. Haines, G. Fraysse, J. Détaint, B. Capelle, and A. Van der Lee, *J. Appl. Phys.* **97**, 074110 (2005).
- ⁴³H. Grimm and B. Dorner, *J. Phys. Chem. Solids* **36**, 407 (1975).
- ⁴⁴W. S. Miller, R. Roy, E. C. Shafer, and F. Dacheille, *Am. Mineral.* **48** (9-1), 1024 (1963).
- ⁴⁵V. S. Balitsky, D. V. Balitsky, A. N. Nekrasov, and L. V. Balitskaya, *J. Phys. IV* **126**, 17 (2005).
- ⁴⁶B. A. Fursenko, V. A. Kirkinsky, and A. P. Rjaposov, *High-Pressure Proceeding Science and Technology Proceedings of the 7th AIRAPT International Conference*, edited by B. Vodar and P. Marteau (Pergamon, Oxford, 1980), p. 562.
- ⁴⁷A. Largeteau, S. Darracq, and G. Goglio, *Z. Naturforsch. B: Chem. Sci.* **63** (6), 739 (2008).
- ⁴⁸E. Angot, R. Le Parc, C. Levelut, M. Beaurain, P. Armand, O. Cambon, and J. Haines, *J. Phys.: Condens. Matter* **18**, 4315 (2006).
- ⁴⁹R. Ouillon, J.-P. Pinan-Lucarre, and P. Ranson, *J. Raman Spectrosc.* **31**, 605 (2000).